

# Optimum Optical Conditions for Fluorescence Imaging Using a Confocal Laser Scanning Microscope to Determine Three-Dimensional Shape of Ink Jet Dots on Paper<sup>1</sup>

Toshiharu Enomae<sup>▲</sup> and Akira Isogai

Graduate School of Agricultural and Life Sciences, The University of Tokyo, Yayoi 1-1-1, Bunkyo-ku, Tokyo 113-8657, Japan

E-mail: E-mail: enomae@psl.fpa.u-tokyo.ac.jp

Mikiko Naito, Yasushi Ozaki and Hisato Nagashima

Research Institute, National Printing Bureau, Sakawa 6-4-20, Odawara Kanagawa 256-0816, Japan

**Abstract.** A nondestructive and simple technique for determining the three-dimensional shape of fixed ink dots was developed, and the optimum conditions of laser excitation and filters to detect fluorescence were determined for both dye and pigment inks for ink jet. Most magenta and black dye inks emit fluorescence at around 580 and 667 nm through laser excitations at 543 and 633 nm, respectively. Yellow dye and pigment inks and a magenta pigment ink were also detected under this condition. The cyan dye ink was excited by 405 nm laser radiation, and the fluorescence was observed by bandpass filtering ranging from 510 to 650 nm discriminately from the paper with no fluorescent brightening agent. Cyan and black pigment inks did not emit detectable fluorescence. Fluorescence emitted from the ink jet inks by laser excitation successfully provided three-dimensional ink distributions with the optical slicing function of a confocal laser scanning microscope. © 2011 Society for Imaging Science and Technology.

[DOI: 10.2352/J.ImagingSci.Technol.2011.55.2.020201]

## INTRODUCTION

The visual appearance of printed images determines the print quality and depends on the morphology of the fixed ink as well as its optical performances. Therefore, the mechanisms of ink penetration and setting are very important for all kinds of printing methods. Unlike pigment inks, dye inks used for ink jet printing have no shape at a visible level after drying, and their distributions cannot be determined by solid morphology. In this work, attention was first paid to fluorescence from dye inks to facilitate the observation of ink geometry—shape, size, location in paper, etc. of ink dots—using a confocal laser scanning microscope (CLSM) in routine analyses.

CLSM application is an efficient and informative tech-

nique for observing ink jet ink distribution. It has also been utilized in other areas of paper science. The most common applications involve geometrical measurements such as surface profiles and fiber network structures. Beland et al.<sup>1</sup> measured the surface profiles of a matte-coated paper three dimensionally using the confocal function and related the perception of gloss to the surface topography. Aggelidis et al.<sup>2</sup> visualized the fiber network deformation caused by calendering to correlate the changes with the macroscopic compressible elastoviscoplastic response of paper coatings. Xu et al.<sup>3</sup> determined paper layer structures from discrete layers created by optical sectioning followed by a dynamic thresholding method for separating fibers from air and artifacts. Enomae et al.<sup>4</sup> calculated the fiber orientation degree for optically sectioned layers of paper. Observation of the trace constituents contained in paper is also within the scope of CLSM.

Khantayanuwong et al.<sup>5</sup> used a CLSM to observe that the unbonded area between fibers of handsheets increased with recycling. Ozaki et al. selectively stained polyamide epichlorohydrin resin in paper with sulforhodamine 101 and observed the resin distribution in the sheet,<sup>6,7</sup> and dyed a latex binder with Rhodamine B to image coating layers.<sup>8,9</sup> Suominen et al.<sup>10</sup> found that bacteria were mainly localized in the interface area between the polyethylene layer and the cellulose fiber web of a food-packaging paperboard stained with acridine orange. Hamada et al.<sup>11</sup> used a CLSM to compare the distributions of aqueous and solvent inks on non-woven sheets, and the hydrophilicity of the fiber surfaces and the dispersion of ink pigment particles were found to determine the evenness of the distributions.

With regard to the analysis of ink penetration into paper, the most popular method involves the cross sectioning of a printed sheet for microscopic observation. This sectioning requires manipulative skills, and it is almost impossible to pinpoint a targeted dot of ink. Microscopic offset ink locations can also be determined by stereoscopic backscatter imaging utilizing scanning electron microscopy.<sup>12</sup> The cross sectioning of a paper sheet with a focused ion beam without

<sup>▲</sup>IS&T Member.

<sup>1</sup>This work was presented in part at the 58th APPITA Annual Conference and Exhibition in Canberra, Australia, April 2004, at IS&T's NIP20: International Conference on Digital Printing Technologies in Salt Lake City, UT, October 2004, and IS&T's NIP23: International Conference on Digital Printing Technologies in Anchorage, AK, September 2007.

Received Oct. 19, 2010; accepted for publication Nov. 11, 2010; published online Mar. 10, 2011.

1062-3701/2011/55(2)/020201/8/\$20.00.

**Table I.** List of ink jet paper samples.

Key	Grade	Basis weight (g/m <sup>2</sup> )	60° gloss
A	Photo quality	295.9	39
B	Photo quality	232.3	32
C	High gloss type	183.5	57
D	Medium	108.6	3
E	Photo quality	261.1	37

any destruction is one of the latest techniques for the clear observation of a thin printed ink layer on paper.<sup>13–15</sup> Time-of-flight secondary ion mass spectrometry is a powerful tool to determine the extent of ink penetration with the element distribution with depth and to create cross-sectional images of a printed sheet.<sup>16,17</sup>

This work introduces a much simpler method for obtaining the three-dimensional (3D) shape of any targeted dot of a magenta or black dye ink without any particular sample preparation skills using a CLSM first. This study explores the extension of this technique to all four primary colors: cyan, magenta, yellow, and black dye and pigment inks in addition to the magenta dye ink.

## EXPERIMENT

### *Paper Samples, Printers, and Inks*

Photo-quality papers A and B, high-gloss-type paper C, and medium-grade paper D, all of which have a silica coating for ink jet, were used. Table I lists the paper samples used. Specular gloss at 60° was measured using a glossmeter (GM-268, Konica Minolta). The mean values in the machine and cross directions are presented in the table. Homogeneous color patterns with a dot area ratio of 10% or 20% were printed on each sheet with magenta and black inks from ink jet printer A.

In order to analyze other inks, commercially available photo-grade glossy paper E was used. A 1-mm-wide line was output onto a paper sheet at a resolution of 600×600 dpi with each of the two ink jet printers B and C. For printer B, cyan, magenta, and yellow inks were dye-based; only the black ink was pigment-based. For printer C, all inks were pigment-based. Each ink was taken out of the ink cartridge to determine the fluorescence properties.

### *Laser Scanning Microscope and Observation*

A CLSM (LSM 510) with an upright body (Axioplan 2, Carl Zeiss, Germany) was utilized. This type of optical microscope obtains 3D images by optical slicing in the thickness direction using the confocal system, employing the power of laser beams to compensate for the resultant insufficient illumination. Laser beams fall on the front side of the sample. The fluorescent light emitted from the fluorescent components of the coloring material included in the ink enters the detector to provide a fluorescence image. A 3D image is reconstructed from a series of digitally accumulated single

**Table II.** Optical condition applied for measuring dye ink dot shape by fluorescence method.

Color of ink jet ink emitting fluorescence	Magenta	Black
Optimum exciting wavelength (nm)	550 (green)	650 (reddish-yellow)
Maximum fluorescence wavelength (nm)	580 (greenish-yellow)	667 (red)
Wavelength of irradiation laser (nm)	543	633
Wavelength of color filter for detection (nm)	560–615	>650
Default pseudocolor in fluorescence image for LSM-510	Red	Blue

confocal images. The magenta and black dye inks from printer A were subjected to observation with the aforementioned system.

A piece of printed sample cut to approximately 15×15 mm<sup>2</sup> was mounted on a slide glass. Next, a drop of fluid paraffin was placed on its corner or edge to allow it to penetrate the sample spontaneously to the other end, leaving as few air bubbles as possible. A cover glass was then mounted on it, and the specimen was subjected to observation. As an impregnation liquid in the case of silica-based ink jet coatings, fluid paraffin was selected because its refractive index is approximately 1.47, which is close to that of silica (approximately 1.45). Less light refraction occurs between substances with closer refractive indices, and even porous materials appear transparent when such a liquid fills the pores.

For observation, the objective lens selected was mainly Plan-Neofluar 40×/0.75. At this magnification, one XY-plane image corresponds to 230.3×230.3 μm<sup>2</sup> with a thickness of a single confocal plane of 0.60 μm. The speed of laser scanning was approximately 30 or 60 s per single image of 1024×1024 pixels. The laser intensity ranged between 30% and 80% of the maximum outputs. The duration of laser irradiation at the same location was as short as 2.3 ms at most if 40 slices were assumed to be accumulated. Therefore, fluorescence degradation could be ignored, although it should be always considered in fluorescent observation. The choice of laser beams was adjusted to the FITC/Rhod/Cy5 mode from the fluorescence probe database. Rhod and Cy5 modes, respectively, suit the magenta and black dye ink dots well for observation. Table II presents a default condition with regard to the wavelength ranges of exciting and fluorescent lights for the magenta and black inks. The ink jet ink dyes appear to have fluorescence properties similar to those registered in the database.

For analyses of cyan and yellow dye inks and all pigment inks, fluorescence images were obtained using another type of CLSM (TCS-SP5, Leica, Germany) equipped with a 63× oil-immersion objective lens (HCX PL APO, numerical aperture of 1.40) that suits an immersion oil with a refractive index of 1.518 supplied by Leica. For observation in the oil-immersion mode, paraffin oil was not applied. Instead, the immersion oil recommended by Leica was applied to

prevent the lens from damage that may be caused by the direct contact with oil. The  $Z$  (thickness) resolution of the oil-immersion lens is improved to less than  $0.6 \mu\text{m}$ , which

is threefold better than that in a lens with air between the sample and the objective lens.<sup>18</sup> Excitation wavelengths of 488 nm specific for an Ar laser and 405 nm from a diode laser were primarily used for observation of the printed paper samples by the CLSM. The pinhole diameter was adjusted to  $151.6 \mu\text{m}$ . Confocal images were obtained using both  $XYZ$  and  $XZY$  scan modes. In the  $XYZ$  mode, a sequence of  $XY$  (plane of the paper) frames was obtained at  $0.15 \mu\text{m}$  intervals in the  $Z$ -direction. In the  $XZY$  mode,  $XZ$  images were obtained through rapid depth scanning. A series of  $XZ$  (paper cross section) frames were taken at  $3.6 \mu\text{m}$  intervals in the  $Y$ -direction. The frame size was  $512 \times 512$  pixels throughout. The measurement time depended on the number of steps and accumulations and the sequential scan mode; it ranged between 3 and 10 min. In most reconstructed images in the following sections, colors of fluorescence are represented in pseudocolors or white for best contrast; these differ from the true colors of emitted fluorescence.

#### Determination of Fluorescence from Ink Jet Inks

To determine the optimum excitation and fluorescence wavelengths, 3D fluorescence spectra of excitation and fluorescence were measured using a fluorescence spectrophotometer (F-2500, Hitachi). The 3D measurement technique was applied to measure the emission spectrum of a sample as the excitation wavelength was scanned. Fluorescence properties were determined with an ink solution of the magenta pigment ink from printer C diluted well with de-ionized water. The fluorescence spectra obtained with other inks were measured using the function of TCS-SC5.

#### Quantitative Dot Shape Analysis

In order to analyze dot shape quantitatively, a relatively large dot of the black dye ink from printer A was formed using a testing ink jet head (HEK-1, Konica-Minolta, Japan) on the general-grade ink jet paper E.

## RESULTS AND DISCUSSION

#### Determination of 3D Structure of Ink Dots

Figure 1 presents example images of ink jet dots composed of four colors: cyan, magenta, yellow, and black acquired using a CLSM. All inks were of the dye type from printer A.

The images on the left and right sides are regular white light reflected images and fluorescence images, respectively. Although the two images were not acquired from the same location, it was found that the magenta ink emits fluorescence in greenish-yellow, the black ink emits fluorescence in red, and neither cyan nor yellow ink emits fluorescence under this optical condition. This observation demonstrated that fluorescence emitted by magenta and black dye inks could be measured to determine the 3D ink dot distribution.

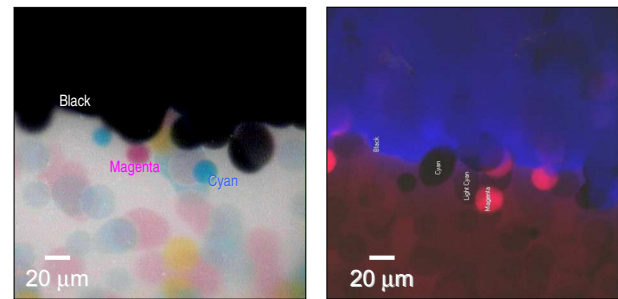


Figure 1. Ink jet dots of cyan, magenta, yellow, and black in reflected light (left) and fluorescence (right) images, not in identical locations. Pre-set pseudocolors are presented for fluorescence. Practically, the blue and red colors represent greenish-yellow and red, respectively.

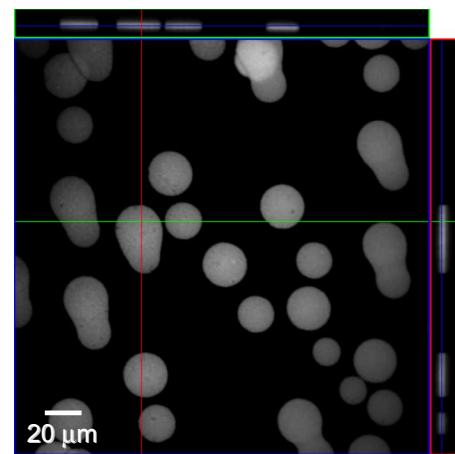
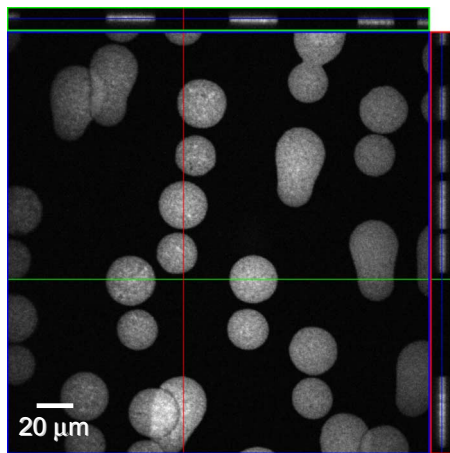


Figure 2. Reconstructed images of magenta ink dots on photo-quality paper A. Greenish-yellow fluorescence emitted by magenta ink is assigned to white to enable clear discernment from the paper background in black.

Dye inks of the same colors used for ink jet printers of other manufacturers were found to exhibit the same fluorescence patterns.

Figures 2 and 3 present reconstructed images of the orthogonal projection for magenta ink dots on photo-quality papers A and B, respectively. In each combined image, the largest (bottom left) picture is the front elevational view in the  $XY$ -plane at height  $Z$ , sectioning the vertical center of most dots. The top picture is for the  $XZ$ -plane

when the sample is sectioned virtually along the horizontal line in the  $XY$ -plane image. The bottom right picture is for the  $YZ$ -plane when the sample is sectioned virtually along the vertical line in the  $XY$ -plane image. In addition to planar dot shape and size, these combined images offer individual dot thickness information from the  $XZ$ - and  $YZ$ -plane images. The thickness is estimated to be constantly approximately  $4 \mu\text{m}$  for both papers. The density distribution inside the dots in the  $XY$ -plane for paper B is less homogeneous than that for paper A, suggesting lower homogeneity of either coating pigment or ink distribution for paper B.



**Figure 3.** Reconstructed images of magenta ink dots on photo-quality paper B. Greenish-yellow fluorescence emitted by magenta ink is assigned to white to enable clear discernment from the paper background in black.

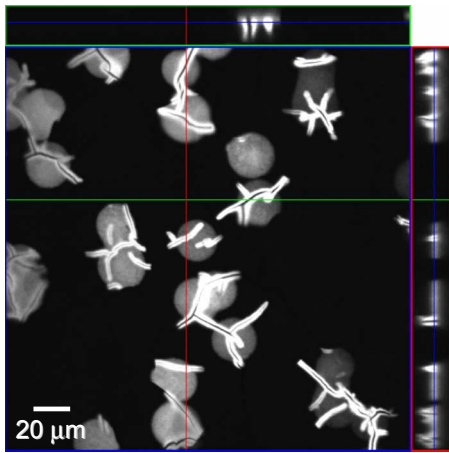


**Figure 4.** Reconstructed images of dye magenta ink dots on high-gloss-type paper C. Greenish-yellow fluorescence emitted by magenta ink is assigned to white to enable clear discernment from the paper background in black.

Figure 4 presents reconstructed images for the high-gloss-type paper C. Bright curved lines are visible around some dots. These are a part of the ink dye that spread over the surfaces of crevices present in the coating surface layer and became concentrated there. Cast coating is often applied to manufacture this gloss-type paper; however, it tends to incur defects such as these surface crevices. The ink appeared to spread over the crevice surfaces twofold to threefold farther than normal penetration, judging from the long bright legs observed in dot cross sections in the XZ- and YZ-planes. This undesirable ink penetration may decrease the color density.

#### Approach to Quantitative Analysis

Figure 5 is a composite image of fluorescent light and transmitted white light for a single dot of the black dye ink on paper D. This image in the XY-plane is one of the 32 slices across which the ink dot extends vertically. The composite image shows that the ink appears to have spread out, avoid-

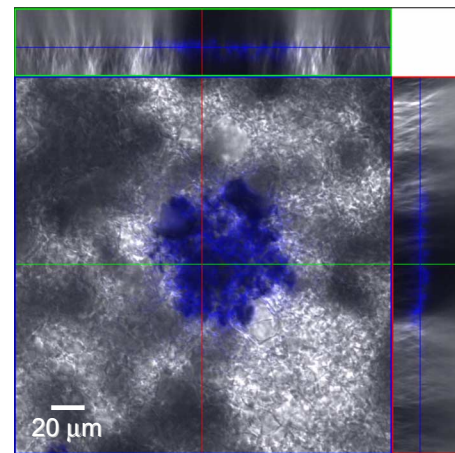


**Figure 5.** Reconstructed images of dye black ink dot on medium-grade paper D in orthogonal projection with the dark (blue) zone indicating black ink dot.

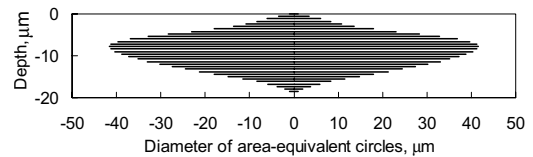


**Figure 6.** Distribution of diameters of circles that are area-equivalent to each slice of optically sectioned dot along the depth from the paper surface for the black dye ink dot shown in the previous figure.

ing large secondary particles of silica. One of the typical problems of CLSM is the attenuation of fluorescence with depth in a 3D image construction. The deeper the location in the sample, the weaker the fluorescence. This is because the laser beam has a longer path to reach a location due to light absorption, scattering, and excitation. Resultant fluorescence also comes through a longer path from that loca-

tion with light absorption and scattering. Fluorescence was previously detected 150  $\mu\text{m}$  below the top surface in the case of uncoated paperboard.<sup>19</sup> Ink dots approximately 20  $\mu\text{m}$  deep appear to emit enough fluorescence to permit image reconstruction.

Figure 6 presents a schematic side view of a black ink dot as a stack of circles that have the same area with an ink region in each slice. Binary images were created for all slices in accordance with the following steps: The threshold level was determined for the central slice by applying discrimination analysis to the Laplacian (secondary differentiation) histogram; the relevant ink dot region within the slice was extracted; and, finally, this procedure was applied to all slices. Xu and Parker<sup>20</sup> applied a method of fitting a curve to the experimental intensity versus depth data and realized an easier and more intimate assessment of cross sections of wood fibers and paper sheets. In our work, however, much less fluorescence reduction was realized to determine locations of ink dot fragments even in deep slices with fluid paraffin that has a refractive index of 1.47 applied to impreg-

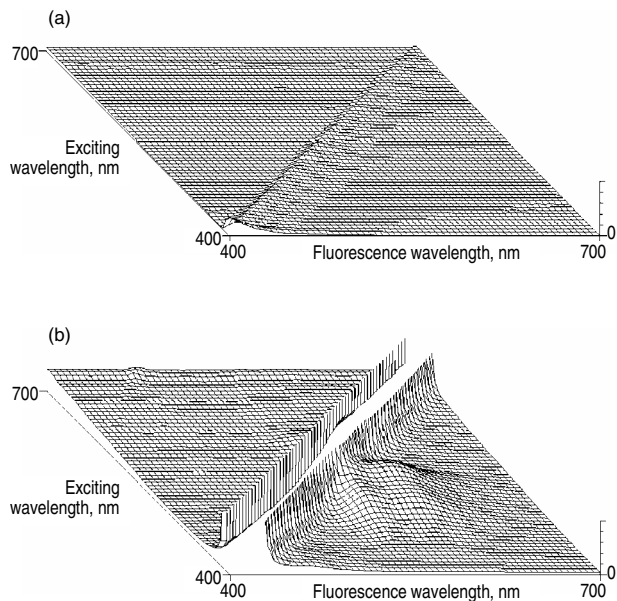


Figure 7. Three-dimensional fluorescence spectra of (a) de-ionized water and (b) magenta pigment ink.

nate coatings to provide improved transparency as well as limited ink location near the surface layer of paper.

In counting the number of pixels, the ink region of each slice was found to have an irregular shape, sometimes having inside holes and small discrete fractions away from the main part. The hole areas were excluded from the ink region, but all discrete fractions were included. The number of pixels

was converted to exact volume in micrometers cubed based on the practical 3D pixel size. In the figure, every circle is shown justified to the center. This 3D area-equivalent stack suggests that the tapering top of the ink dot derives from surface roughness, and the tapering bottom derives from inhomogeneous ink penetration with feathering. The largest circle is located slightly higher than the through-thickness center, meaning that longer feathering occurred during the ink penetration to a greater extent than the surface roughness level.

#### Pigment Inks and Dye Inks for Ink Jet

Figure 7 presents the 3D fluorescence spectra of the de-ionized water and the magenta pigment ink from printer C. The linear raised part in the center does not indicate fluorescence; it simply shows the reflection of exciting (illuminating) light. Compared to the spectrum of water with no fluorescence emission observed [Fig. 7(a)], the magenta ink had fluorescence on wavelengths between 550 and 600 nm for the excitation wavelength range from 500 to 580 nm [Fig. 7(b)].

Figures 8 and 9 present the fluorescence spectra of dye and pigment inks, respectively. The most efficient excitation wavelength (405 or 488 nm) was selected for each ink from the several diode laser wavelengths. Each spectrum is presented in reference to the highest fluorescence response in the spectrum. The magenta and yellow of both dye and pigment inks emit fluorescence at an excitation wavelength of

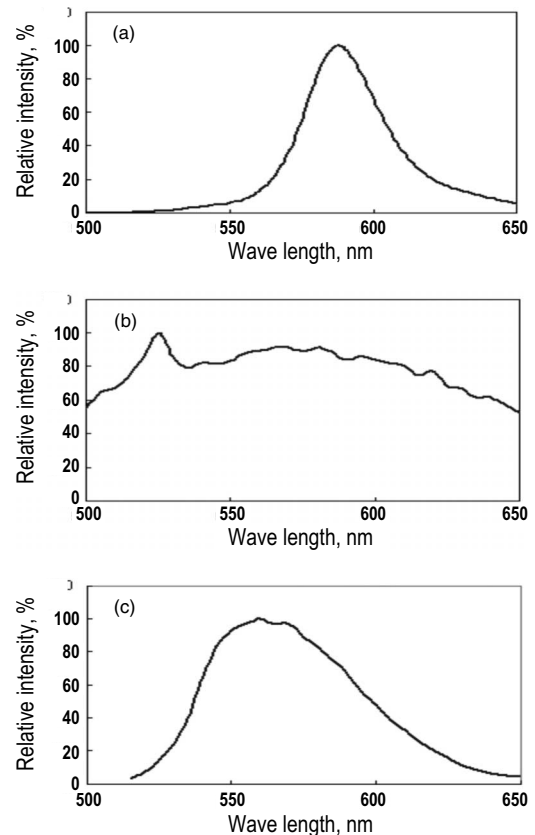


Figure 8. Fluorescence spectra of dye inks: (a) magenta at excitation wavelength of 488 nm, (b) yellow at excitation wavelength of 488 nm, and (c) cyan at excitation wavelength of 405 nm.

488 nm. The magenta dye exhibited a strong fluorescence peak at around 590 nm, which is close to the maximum fluorescence wavelength already known, as shown in Table II. The magenta pigment ink exhibited two peaks at 548 and 590 nm as shown in Fig. 9(a). The yellow dye ink exhibited a small peak at around 525 nm. The yellow pigment ink exhibited a broad fluorescence peak at around 550 nm as

shown in Figs. 8(b) and 9(b), respectively. The cyan inks exhibited a fluorescence peak at around 460 nm for the dye ink and at around 480 nm for the pigment ink, both at an excitation wavelength of 405 nm, as shown in Figs. 8(c) and 9(c), respectively. Black pigment inks from both printers B and C exhibited no fluorescence at any excitation wavelength, although the black dye ink exhibited a clear fluorescence, as mentioned in the previous section. Black pigments commonly consisting of carbon black have no chromophores; however, black dye inks consist of mixed several dyes, one or some of which have chromophores.

Figure 10 presents reconstructed images of the yellow dye ink printed samples that were obtained in the XYZ scan mode of the CLSM. The deepest ink penetration depth of each dot was evaluated to range between 6 and 11  $\mu\text{m}$  from dot to dot, resulting in widely distributed penetration. Consequently, the inks tended to penetrate more deeply as the diameter of the ink dot increased. Within one ink dot, the ink appears to have penetrated more deeply in the central

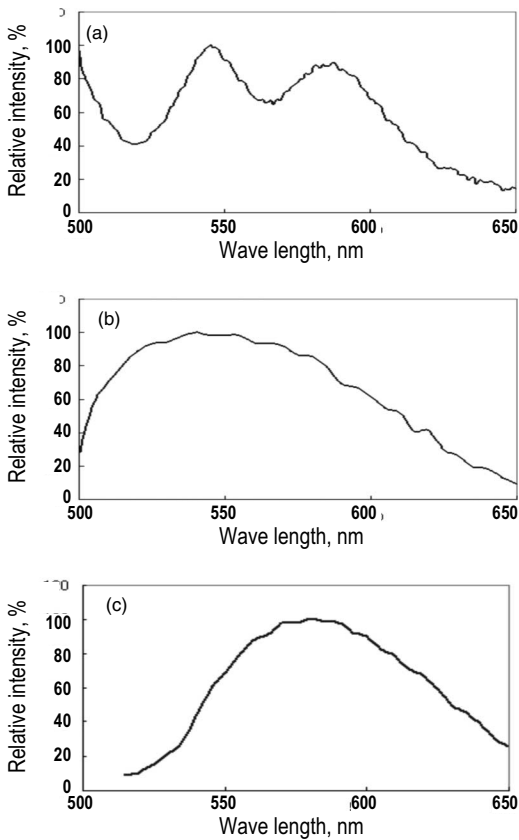


Figure 9. Fluorescence spectra of pigment inks: (a) magenta at excitation wavelength of 488 nm, (b) yellow at excitation wavelength of 488 nm, and (c) cyan at excitation wavelength of 405 nm.

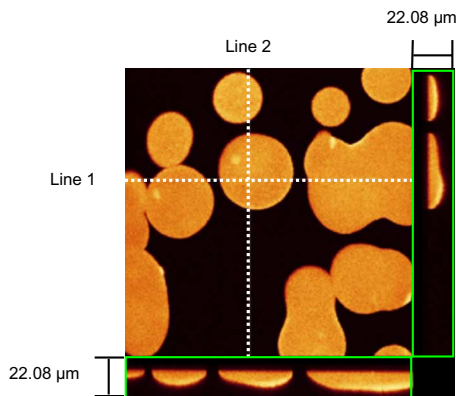


Figure 10. Reconstructed images of yellow dye ink dots on paper F obtained in the XYZ scan mode of CLSM.

part than in the peripheral part, in contrast to the tendency found in Figs. 2 and 3. This appears to be due to the absence of an ink fixing layer on the top of ink jet paper E only or the lower speed of lateral spreading of an ink drop on the surface of ink jet paper E.

Figure 11 presents an XZ-plane image of the cyan dye ink printed sample that was obtained directly in the XZY scan mode instead of the regular XYZ scan mode. The XZY scan mode was chosen because fluorescence from the cyan

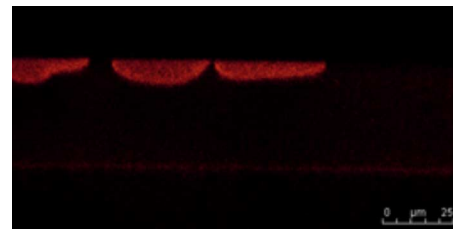


Figure 11. Reconstructed image of cyan dye ink dots on paper E obtained in the XZY scan mode of CLSM.

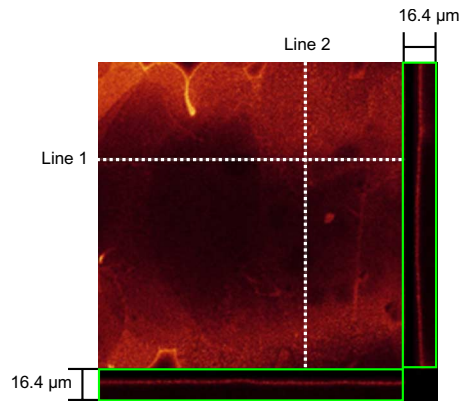


Figure 12. Reconstructed images of magenta pigment ink dots on paper E obtained in the XYZ scan mode of CLSM.

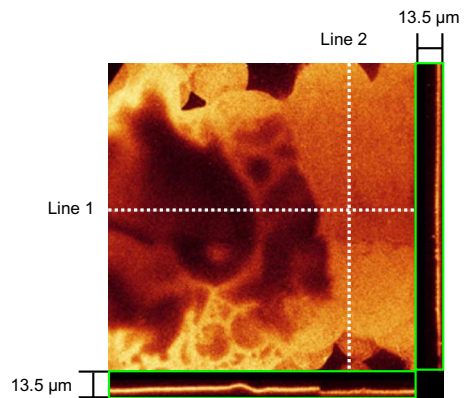


Figure 13. Reconstructed images of yellow pigment ink dots on paper E obtained in the XYZ scan mode of CLSM.

dye ink might be degraded by laser irradiation for the duration of scanning. This technique seems to be effective for coloring materials that tend to lose fluorescence properties rapidly. The cyan dye ink in the glossy photo-ink jet paper could be well observed by the CLSM because it maintained sufficient fluorescence intensity, and the ink jet paper had no competitive fluorescence. In the case of commercial wood-free paper or common ink jet paper, however, the cyan dye ink could not be observed successfully because the optical brightening agents contained in the paper emitted strong fluorescence at the excitation wavelength of 405 nm.

Figure 12 presents reconstructed images for the magenta

**Table III.** Optimum conditions of exciting wavelength and optical filter wavelength.

Ink	Optimum exciting laser wavelength(nm)	Optical filter wavelength range(nm)
Cyan dye ink	405	420–550
Cyan pigment ink	Not available	Not available
Magenta dye ink (1)	543	560–615
Magenta dye ink (2)	488	510–650
Magenta pigment ink	488	510–650
Yellow dye ink	488	510–650
Yellow pigment ink	488	510–650
Black dye ink	633	>650
Black pigment ink	Not available	Not available

pigment printed sample obtained in the XYZ scan mode of the CLSM. In comparison with the common light-reflection microscopic image at the same location, it was confirmed that the distribution of the ink pigment fixed on the ink jet paper appeared sharp in the fluorescence images. The fluorescence spectrum in Fig. 8(a) suggests that there are two fluorescent chromophore groups or compounds present in

the ink. It is known that the ink-receptive layer of the paper emitted neither fluorescence corresponding to the two peaks. Therefore, these fluorescence properties resulted in the distinguished images, although the relation with the molecular structure could not be discussed any further because the chromophore chemical structures and even Color Index numbers of all the inks are disclosed by the manufacturers.

Figure 13 presents the reconstructed images for the yellow pigment printed sample obtained in the XYZ scan mode. The thickness of the ink layer was estimated to be approximately 4  $\mu\text{m}$  from the full Z-depth of 13.5  $\mu\text{m}$ . This thickness of the ink layer located limitedly near the surface was estimated to be lower than those of the yellow and cyan dye inks, as Desie et al.<sup>21</sup> clarified that the pigment-based inks create pigment filter cakes by aggregation of pigment particles on the top of the surface at initial imbibitions.

A cyan pigment printed sample was searched for fluorescence, but appropriate optical conditions could not be found to discriminate it from paper. This is presumably because the absolute fluorescence intensity of the ink was very low, although the peak observed in Fig. 8(c) appears relatively intense. Consequently, this cyan pigment ink fixed on paper was one of the two inks that could not be observed by the CLSM (the other was the black pigment ink).

#### Optical Conditions of Laser and Filter Wavelengths

Table III lists the optimum conditions for the combination of wavelength between laser irradiation and optical bandpass filter to observe the dye and pigment inks using a CLSM obtained from the experiments thus far. The Leica microscope permits one to select the exciting wavelength and configure filter wavelengths arbitrarily and independently, while the Carl-Zeiss microscope permits one to select the combi-

nation from several default patterns. Therefore, there were differences in the wavelength between the two microscopes. Although these conditions are expected to apply to many other kinds of inks of the same color for an ink jet, they will not apply to every ink.

#### CONCLUSIONS

Most magenta and black dye inks for ink jets emit fluorescence at around 580 and 667 nm by laser excitations at 543 and 633 nm, respectively. These fluorescence properties are useful for providing three-dimensional ink distributions using a confocal laser scanning microscope. In applications to ink jet papers, the shape of ink dots on photo-quality paper, cast-coated high-gloss paper, and medium-grade paper was coinlike with a constant thickness, extensional due to spread over crevice surfaces, and rough with rugged edges, respectively. Three-dimensional image analysis applied to a single ink dot resulted in the largest cross section located slightly higher than the thickness center. Extension of this method was attempted using other inks. It was found that the method is applicable to all colors of dye and pigment inks except cyan pigment and black pigment inks. The cyan dye ink was excited by a 405 nm laser and could be observed discriminately from the paper with no fluorescent brightening agent. The magenta and yellow dye and pigment inks were excited by a 488 nm laser and were observed successfully.

#### ACKNOWLEDGMENTS

The authors wish to thank Kazumasa Matsumoto and Kenzo Nakanishi of the Konica Minolta Technology Center, Japan for permitting us to use the testing ink jet head and Fumihito Fujimaki of Nakagawa Manufacturing Co., Ltd., Japan for supplying ink jet printing paper samples.

#### REFERENCES

- <sup>1</sup>M. C. Beland, S. Lindberg, and P. A. Johansson, "Optical measurement and perception of gloss quality of printed matte-coated paper", *J. Pulp Pap. Sci.* **26**, 120 (2000).
- <sup>2</sup>C. N. Aggelidis, M. Pasquali, and L. E. Scriven, "Calendering: Rheology, computations, and experiments", *Proc. of the 13th Int. Congress on Rheology* (British Society of Rheology, Glasgow, 2000) Vol. **3**, p. 425.
- <sup>3</sup>L. Xu, I. Parker, and C. Osborne, "Technique for determining the fibre distribution in the z-direction using confocal microscopy and image analysis", *Appita J.* **50**, 325–328 (1997).
- <sup>4</sup>T. Enomae, Y.-H. Han, A. Isogai, M. Hotate, and S. Hasegawa, "Mechanisms of perception of laid lines in Japanese paper", *J. of Wood Science* **56**, 395 (2010).
- <sup>5</sup>S. Khantayanuwong, T. Enomae, and F. Onabe, "Effect of fiber hornification in recycling on bonding potential at interfiber crossings: Confocal laser-scanning microscopy", *Tappi J.* **56**, 79–85 (2002).
- <sup>6</sup>Y. Ozaki, "The observation of wet-strength resin in the paper by the confocal laser scanning microscope", *Fibers preprints, JAPAN* **58**, 176 (2003) (in Japanese).
- <sup>7</sup>Y. Ozaki, D. W. Bousfield, and S. M. Shaler, "The characterization of polyamide epichlorohydrin resin in paper—Relationship between beating degree of pulp and wet strength", *Appita J.* **59**, 326–329 (2003).
- <sup>8</sup>Y. Ozaki, D. W. Bousfield, and S. M. Shaler, "Observation of the ink penetration into coated paper by confocal laser scanning microscope", *TAGA J.* **3**, 51–59 (2006).
- <sup>9</sup>Y. Ozaki, D. W. Bousfield, and S. M. Shaler, "Three-dimensional observation of coated paper by confocal laser scanning microscope", *Tappi J.* **5**, 3–8 (2006).
- <sup>10</sup>I. Suominen, M.-L. Suihko, and M. Salkinoja-Salonen, "Microscopic

- study of migration of microbes in food-packaging paper and board”, *J. Ind. Microbiol. Biotechnol.* **19**, 104–113 (1997).
- <sup>11</sup> H. Hamada, D. W. Bousfield, and W. T. Luu, “Absorption mechanism of aqueous and solvent inks into synthetic nonwoven fabrics”, *J. Imaging Sci. Technol.* **53**, 050201 (2009).
- <sup>12</sup> T. Helle and P. O. Johnsen, “Using stereoscopic and SEM backscatter imaging for studying ink distribution details on paper and fiber surfaces”, *J. Pulp Pap. Sci.* **20**, 189–192 (1994).
- <sup>13</sup> H. Uchimura and M. Kimura, “A sample preparation method for paper cross-sections using a focused ion beam”, *Sen’i Gakkaishi* **54**, 360–366 (1998) (in Japanese).
- <sup>14</sup> H. Uchimura, “Preparation method of paper and printed paper cross-sections using a focused ion beam to observe it with microscope”, *Nihon Gazo Gakkaishi (J. of the Imaging Society of Japan)* **42**, 168–172 (2003) (in Japanese).
- <sup>15</sup> H. Uchimura, Y. Ozaki, and M. Kimura, “Observation of dyed ink penetrated into ink jet printing paper”, *J. of Printing Science and Technol.* **38**, 216–224 (2001) (in Japanese).
- <sup>16</sup> J. Pinto and M. Nicholas, “SIMS studies of ink jet media”, in *Recent Progress in Ink Jet Technologies II* (IS&T, Springfield, VA, 1999), pp. 383–389.
- <sup>17</sup> M. Shibatani, T. Asakawa, T. Enomae, and A. Isogai, “Approach for detecting localization of inkjet ink components using dynamic-SIMS analysis”, *Colloids Surf., A* **326**, 61–66 (2008).
- <sup>18</sup> E. H. K. Sterlzer, *Handbook of Biological Confocal Microscopy* (Plenum, New York, 1995), pp. 139–153.
- <sup>19</sup> T. Enomae, Y.-H. Han, and A. Isogai, “Z-Directional distribution of fiber orientation of Japanese and western papers determined by confocal laser scanning microscopy”, *J. of Wood Science* **54**, 300–307 (2008).
- <sup>20</sup> L. Xu and I. Parker, “Correction of fluorescence attenuation with depth in fibre and paper images collected by confocal laser scanning microscopy”, *Appita J.* **52**, 41–44 (1999).
- <sup>21</sup> G. Desie, G. Deroover, F. De Voeght, and A. Soucemarianadin, “Printing of dye and pigment-based aqueous inks onto porous substrates”, *J. Imaging Sci. Technol.* **45**, 389–397 (2004).